JOURNAL OF COMPUTATIONAL PHYSICS 101, 419–430 (1992)

# Time Domain Numerical Calculations of Unsteady Vortical Flows about a Flat Plate Airfoil

S. I. HARIHARAN* AND YU PING

*Department of Mathematical Sciences, University of Akron, Akron, Ohio 44325*

AND

J. R. SCOTT

*NASA Lewis Research Center, Cleveland, Ohio 44135*

Received September 7, 1989; revised January 27, 1991

A time domain numerical scheme is developed to solve for the unsteady flow about a flat plate airfoil due to imposed upstream, small amplitude, transverse velocity perturbations. The governing equation for the resulting unsteady potential is a homogeneous, constant coefficient, convective wave equation. Accurate solution of the problem requires the development of approximate boundary conditions which correctly model the physics of the unsteady flow in the far field. An accurate far field boundary condition is developed, and numerical results are presented using this condition. The stability of the scheme is discussed, and the stability restriction for the scheme is established as a function of the Mach number. Finally, comparisons are made with the frequency domain calculations by Scott and Atassi, and the relative strengths and weaknesses of each approach are assessed. © 1992 Academic Press, Inc.

## 1. INTRODUCTION

In recent years, due to the availability of large high speed computers and improvements in numerical algorithms, much progress has been made by computational fluid dynamicists in the effort to solve unsteady aerodynamic flow problems. To date most numerical work in unsteady aerodynamics has concentrated on either potential or primitive variable methods. The early work goes back to the 1970s when researches developed methods to solve the unsteady small disturbance potential equation for flows around oscillating airfoils or cascades. Later work concentrated on solving the unsteady full potential equation or the linearized unsteady potential equation. Unsteady potential methods have proven to work well for oscillating airfoil problems, and much effort has been expended in their development. References [1–5] represent some of the work that has been done in this area.

The biggest drawback associated with unsteady potential methods is that they are not suitable for the solution of vortical flow problems. Previous efforts to use the small disturbance potential formulation to analyze unsteady vortical flows around airfoils have assumed that the upstream vorticity is convected at uniform speed and not distorted in any way by the gradients in the mean flow. McCroskey and Goorjian [6] and McCroskey [7] have reported such an approach, in which the well-known unsteady, transonic small-disturbance code LTRAN2 was modified to handle imposed sinusoidal vortical gusts. However, as shown by Goldstein and Atassi [8] and Atassi [9], the assumption that the gust is convected at uniform velocity and not distorted by the mean flow is only valid for flat plate airfoils. For airfoils with thickness, camber, or angle of attack, there are gradients in the mean flow which act to distort the structure of the convected vortical gust. The results of Goldstein and Atassi [8] and Atassi [9], as well as the recent numerical results of Scott [10, 11], have shown that the effects of mean flow distortion on the unsteady velocity field are very strong, and can lead to large changes in the unsteady solution. Since turbomachinery flow fields are characterized by strong mean flow gradients, any numerical scheme which is developed for these flow fields will not be accurate unless it takes into account the distortion of the convected upstream vorticity.

More recently, with the increasing availability of faster and larger computers, researchers have been developing the so-called primitive variable methods in which the unsteady Euler or Navier–Stokes equations are solved in time along with certain specified boundary conditions. Whereas the

* Research partially supported by NASA while the first author was visiting ICOMP, NASA Lewis Research Center and by the Ohio Supercomputer Center, Columbus, Ohio.



0021-9991/92 $5.00

potential methods are essentially limited to oscillating airfoil problems, the primitive variable methods are equally well-suited to both oscillating airfoil and vortical flow problems. However, these methods suffer the disadvantage of being too expensive to use for routine engineering calculations such as are encountered in design work. In addition, and perhaps most importantly, uncertainties about physically correct far field boundary conditions and difficulties in resolving multiple time scales such as are encountered in high speed vortical flows leave some question as to the accuracy of the solutions.

For many aerodynamic flows of practical interest, the unsteadiness in the flow arises due to the occurrence of small, upstream vortical disturbances (gusts) which are convected downstream and interact with an airfoil or cascade of airfoils. Since the time scale associated with these small amplitude disturbances is usually an order of magnitude greater than the time scale associated with the basic mean flow, the dominant unsteady effects in the flow will be due to the high speed convection of the upstream unsteady disturbances. For this kind of "weakly rotational" flow, it is possible to use an alternative to the nonlinear primitive variable approach known as the "rapid distortion approximation." Mathematically, this amounts to linearizing the unsteady Euler equations about the basic nonlinear steady flow field and then solving the resulting time linearized governing equations.

Goldstein [12] and Atassi and Grzedzinski [13] have shown that for potential mean flows, it is possible to reduce the mathematical problem for the unsteady flow to solving a single, nonconstant-coefficient convective wave equation. Their formulation of the problem fully accounts for the distortion of the convected upstream vorticity by the gradients in the nonuniform mean flow, and therefore represents a major improvement over the traditional unsteady potential formulation.

Scott and Atassi [10, 14, 15] have recently reported the development of a numerical scheme which implements this linearized approach for the purpose of solving unsteady vortical flows around lifting airfoils. Their method solves the problem in the frequency domain and has been validated for compressible subsonic flows for a large range of reduced frequencies. Their numerical scheme can also be used for the solution of irrotational flows such as are encountered in the oscillating airfoil problem. Because of the inherent efficiency of their linearized approach and its ability to correctly handle both vortical and non-vortical unsteady flows, their approach represents an attractive alternative to the potential and primitive variable methods for the solution of unsteady aerodynamic flow problems.

An alternative to the frequency domain approach would be to solve the linearized problem using a time domain formulation. The time domain approach is of interest for a number of reasons. First, since the full nonlinear unsteady Euler equations are solved using time marching methods, there is considerable theoretical interest in the study of time marching methods to solve their linearized counterpart. Second, the development and analysis of far field boundary conditions for the linearized unsteady problem has a direct bearing on the use of far field boundary conditions for the nonlinear problem. Finally, for certain problems the time domain approach may offer some advantages over the frequency domain approach. For example, the frequency domain approach is limited to solving the gust response problem for a single frequency and then superposing solutions for more general disturbances in which multiple frequencies are present. For vortical disturbances that contain a large number of harmonics, many calculations would be necessary and the frequency domain approach would be inefficient. The time domain approach, however, could handle the multiple frequency case in a single calculation and could possibly be more efficient in this case.

Our major purpose in the present paper is to present a time domain numerical scheme for the solution of unsteady vortical flows around thin airfoils. The numerical procedure that we present is designed specifically for the linearized problem and is second-order accurate in both time and space. While it is possible to modify previous time domain, unsteady potential formulations, such as the one by Engquist and Osher [16], to apply to the present linear problem, we point out that these schemes were developed to solve the transonic small disturbance equation which is a nonlinear equation. Also, these schemes were designed to capture shocks and used appropriate upwinding techniques which would unnecessarily complicate the solution of the present linear problem. Since in the present approach the nonlinear mean flow is calculated first, and then the unsteady flow is determined as a first-order perturbation about the mean flow, it is not necessary to use a shock-capturing algorithm for the unsteady part of the problem. In addition, the numerical schemes that have been developed to solve unsteady potential flows are generally only first-order accurate in time, whereas the present approach is second-order accurate [1, 17].

For simplicity, the numerical scheme which we present in this paper has been developed for the thin airfoil problem in which the mean flow is a uniform parallel flow. However, the extension of our method to flows with real geometry effects in which the mean flow is no longer uniform is relatively straightforward. In Section 2 we derive the linearized equations and formulate the boundary value problem for the special case of a thin airfoil. In Section 3 the far field boundary condition is derived, and in Section 4 the basic numerical scheme is presented. Section 5 discusses the details of the calculation of the unsteady response function, and in Section 6 we discuss computed numerical results and compare them with the results of Scott and Atassi as reported in [14].

## 2. FORMULATION OF THE PROBLEM

### 2.1. *Derivation of Governing Equation*

The formulation that is presented here follows that given in the recent review paper of Atassi [18]. Consider the equations of fluid motion for an ideal gas which is inviscid and non-heat conducting. The governing continuity, momentum, and entropy equations may be written

$$\rho_t + \nabla\cdot(\rho\mathbf{v}) = 0 \tag{1}$$

$$\mathbf{v}_t + (\mathbf{v}\cdot\nabla)\,\mathbf{v} + \frac{1}{\rho}\nabla p = 0 \tag{2}$$

$$s_t + \mathbf{v}\cdot\nabla s = 0, \tag{3}$$

where $\rho$, $\mathbf{v}$, $p$, and $s$ are the fluid density, velocity, pressure, and entropy, respectively.

This is a system of nonlinear equations. Since we assume that the upstream vortical disturbances are small compared to the mean velocity, we linearize about the mean flow state and introduce perturbation quantities as follows: Let

$$\rho = \rho_0 + \varepsilon\tilde{\rho} \tag{4}$$

$$\mathbf{v} = \mathbf{v}_0 + \varepsilon\mathbf{u} \tag{5}$$

$$p = p_0 + \varepsilon\tilde{p} \tag{6}$$

$$s = s_0 + \varepsilon\tilde{s}, \tag{7}$$

where $\varepsilon$ is small compared to the corresponding zeroth-order quantities that govern the mean flow whose density, velocity, pressure, and entropy are $\rho_0$, $\mathbf{v}_0$, $p_0$, and $s_0$, respectively.

In the case of thin airfoils at zero mean incidence, the mean velocity is a uniform parallel flow in the $x$ direction, so that $\mathbf{v}_0 = v_0\mathbf{e}_x$. The first-order asymptotic expansion ($O(\varepsilon)$) is thus

$$\frac{1}{\rho_0 c_0^2}\left(\frac{\partial}{\partial t} + v_0\frac{\partial}{\partial x}\right)\tilde{p} = -\nabla\cdot\mathbf{u} \tag{8}$$

$$\rho_0\left(\frac{\partial}{\partial t} + v_0\frac{\partial}{\partial x}\right)\mathbf{u} = -\nabla\tilde{p} \tag{9}$$

$$\left(\frac{\partial}{\partial t} + v_0\frac{\partial}{\partial x}\right)\tilde{s} = 0, \tag{10}$$

where $c_0 = \sqrt{\gamma p_0/\rho_0}$ is the acoustic speed.

Following the traditional splitting of the unsteady velocity into solenoidal and irrotational components [18], let

$$\mathbf{u} = \mathbf{u}_1 + \nabla\phi, \tag{11}$$

where $\mathbf{u}_1$ satisfies

$$\nabla\cdot\mathbf{u}_1 = 0 \tag{12}$$

and

$$\left(\frac{\partial}{\partial t} + v_0\frac{\partial}{\partial x}\right)\mathbf{u}_1 = 0. \tag{13}$$

Using Eqs. (11) and (13) in (9), there results

$$\rho_0\left(\frac{\partial}{\partial t} + v_0\frac{\partial}{\partial x}\right)\nabla\phi = -\nabla\tilde{p} \tag{14}$$

or

$$\rho_0\left(\frac{\partial}{\partial t} + v_0\frac{\partial}{\partial x}\right)\phi = -\tilde{p} + f(t),$$

where $f(t)$ is an arbitrary function of $t$. At upstream infinity $\phi$, $\phi_x$, and $\tilde{p}$ vanish. From this we deduce that

$$\rho_0\left(\frac{\partial}{\partial t} + v_0\frac{\partial}{\partial x}\right)\phi = -\tilde{p}. \tag{15}$$

Substituting (15) into (8) and using (11) one obtains

$$\left(\frac{\partial}{\partial t} + v_0\frac{\partial}{\partial x}\right)^2\phi = c_0^2\nabla^2\phi. \tag{16}$$

Equation (16) is the governing equation for the unsteady potential for the problem of small vortical disturbances to a uniform flow past a flat plate airfoil.

The total velocity field $\mathbf{v}$ is given by

$$\mathbf{v} = v_0\mathbf{e}_x + \mathbf{u}_1 + \nabla\phi. \tag{17}$$

We observe that once the potential field is determined, the pressure and the velocity are determined from Eqs. (15) and (17), respectively.

### 2.2. *Boundary Conditions*

Now consider the problem of flow past a flat plate airfoil at zero degrees mean incidence with small amplitude, unsteady velocity disturbances imposed upstream (see Fig. 1). The mean flow is a uniform parallel flow in the $x$ direction, and the $y$ direction is taken to be perpendicular to the airfoil. Now from conditions (12) and (13) we conclude that $\mathbf{u}_1$ must be of the form

$$\mathbf{u}_1 = \mathbf{u}_1(x - v_0 t, y) \tag{18}$$


FIG. 1. Flat plate Airfoil in a transverse gust.

and that the upstream disturbances are convected by the mean flow. Here

$$\mathbf{u}_1 = w\mathbf{e}_x + v\mathbf{e}_y, \tag{19}$$

where $w$ and $v$ must be chosen to satisfy the divergence free condition (12). The unsteady velocity $\mathbf{u}$ must satisfy $\mathbf{u} \to \mathbf{u}_1$ as $x \to -\infty$. Therefore $\phi$ must satisfy

$$\nabla\phi \to 0 \qquad \text{as} \quad x \to -\infty. \tag{20}$$

At the airfoil surface, the normal component of the velocity must vanish. This leads to the requirement that

$$v + \frac{\partial}{\partial y}\phi = 0. \tag{21}$$

In the wake behind the airfoil $\phi$ is not continuous but must satisfy a jump condition determined by the continuity of the unsteady pressure. Applying (15) on each side of the vortex sheet behind the airfoil leads to the condition

$$\left(\frac{\partial}{\partial t} + v_0\frac{\partial}{\partial x}\right)\Delta\phi = 0, \tag{22}$$

where $\Delta\phi$ is the jump in $\phi$ across the wake.

### 2.3. *Nondimensionalization of the Problem*

For computational purposes it is convenient to non-dimensionalize the problem. We therefore introduce the following normalization. Let

$$T = \frac{v_0}{l/2}\,t \tag{23}$$

$$X = \frac{x}{l/2} \tag{24}$$

$$Y = \frac{y}{l/2} \tag{25}$$

$$c = \frac{c_0}{v_0}. \tag{26}$$

In the above nondimensionalization, $l$ is the chord length of the airfoil. Denoting $T$, $X$, $Y$ by $t$, $x$, and $y$ again, respectively, the problem takes the form

$$\frac{\partial^2\phi}{\partial t^2} + 2\frac{\partial^2\phi}{\partial t\,\partial x} + \frac{\partial^2\phi}{\partial x^2} = c^2\nabla^2\phi \qquad \text{governing equation} \tag{27}$$

$$\frac{\partial}{\partial t}\Delta\phi + \frac{\partial}{\partial x}\Delta\phi = 0 \qquad \text{in the wake} \tag{28}$$

$$v + \frac{\partial}{\partial y}\phi = 0 \qquad \text{airfoil surface} \tag{29}$$

$$\nabla\phi \to 0 \qquad \text{as} \quad x \to -\infty. \tag{30}$$

Note that the quantity $c$ is now the inverse Mach number of the mean flow.

## 3. ABSORBING BOUNDARY CONDITIONS

The boundary value problem prescribed in Eqs. (27)–(30) is an open domain problem. In order to obtain numerical solutions to this problem it is necessary to truncate the domain onto a finite region as shown in Fig. 2. Because we consider only flat plate airfoils with zero thickness, the solution $\phi$ is an odd function with respect to $y$. Therefore it is only necessary to solve the problem in the upper half plane. The computational domain is the rectangular region defined by $[-L, L] \times [0, H]$.

Because the open domain problem has been truncated onto a finite region with fixed boundaries and since the gust response problem is essentially a wave propagation problem, it is necessary to derive far field boundary conditions which allow outgoing acoustic waves to pass through the far field boundary without being reflected back into the computational domain. Since the governing equation is a convective wave equation, and not the regular wave equation, there are difficulties in deriving nonreflecting far field boundary conditions. We shall present an approach due to [22] which is used in our computations, and we will now describe this approach in detail.

Generalization of the ideas to follow are found in Hariharan and Hagstrom [22]. This procedure has

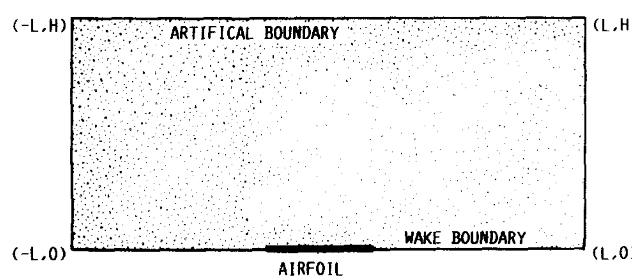


FIG. 2. Computational domain.

similarities to that of Bayliss and Turkel [20], but is obtained through a systematic derivation and has general validity. The condition which is developed in [20] was used for prescribing an outflow condition, whereas the conditions developed in [22] are valid on the entire far field boundary.

To present the ideas, we consider the convective wave equation (27). The idea has both a geometrical and an algebraic point of view. The geometrical view is that we seek a transformation in which the waves at infinity are cylindrical with respect to a moving source convected along the $x$ axis with a speed unity. We shall now describe this process.

Suppose we consider a wave front at a time $t = t^*$. From time $t = 0$ to this time a source in the flow is convected a distance $t^*$. The signals would have propagated to a distance $ct^*$. Thus the first step in deriving the transformation we seek is to develop a relation between $t^*$ and $ct^*$ with respect to a fixed observer. This is depicted in Fig. 3.

In this figure, if we label the distance from the origin to the wave front by $\hat{R}t^*$, we obtain

$$\hat{R}^2 + 1 - 2\hat{R}\cos\theta = c^2. \tag{31}$$

Solving for $\hat{R}$ we obtain

$$\hat{R}(\theta) = \cos\theta \pm \sqrt{c^2 - \sin^2\theta}. \tag{32}$$

We conclude on the basis of the behavior near $\theta = 0$ and $\theta = \pi$ that only the positive sign is valid.

Thus the desired transformation in which the cylindrical properties are obtained is

$$\hat{r} = \frac{r}{\hat{R}(\theta)}, \qquad \hat{\theta} = \theta. \tag{33}$$

The interpretation is that at $r = \hat{R}(\theta)\, t^*$, $\hat{r} = t^* =$ constant, the wave front is cylindrical.

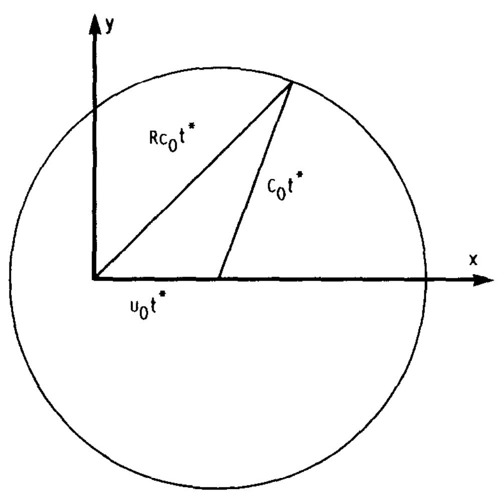


**FIG. 3.** Wave front with respect to a moving source.

Now in the new coordinate system $(\hat{r}, \hat{\theta})$, which we call the wave front coordinate system, one can represent the solution in the far field following Friedlander [7] in an asymptotic form. That is,

$$\phi \sim \frac{f(t - \hat{r}, \theta)}{\hat{r}^{1/2}}. \tag{34}$$

From this, we obtain a radiation boundary condition that is similar to the one that is reported in [1], which is

$$\phi_t + \phi_{\hat{r}} + \frac{\phi}{2\hat{r}} = O(\hat{r}^{-5/2}). \tag{35}$$

Thus the desired boundary condition is a translation of (35) in the original coordinate system. This results in the boundary condition

$$S(\theta)\,\phi_t + \phi_r + \frac{\phi}{2r} = 0, \tag{36}$$

where $S(\theta) = 1/\hat{R}(\theta)$. This condition is implemented in the results reported in the present paper. The origin is chosen to be the center of the airfoil. In the numerical calculations this is implemented as

$$\phi_t + \frac{1}{S(\theta)}\,[\cos(\theta)\,\phi_x + \sin(\theta)\,\phi_y] + \frac{\phi}{2rS(\theta)} = 0. \tag{37}$$

We remark here that, in contrast to the geometric derivation given above, the transformation (32) can also be obtained algebraically by solving the Eikonal equation corresponding to (27) which is

$$1 - 2\sigma_x + \sigma_x^2 = c^2(\sigma_x^2 + \sigma_y^2).$$

## 4. NUMERICAL SCHEME AND STABILITY

### 4.1. *Basic Scheme and the Stability Constraint*

The indices used in our numerical calculations are $i$ and $j$, where $i$ varies from 0 to $M$ along the $x$ axis and $j$ varies from 0 to $N$ along the $y$ axis. The index $n$ is used to denote values as the time $n\,\Delta t$, where $\Delta t$ is the time step. The grid spacing in the $x$ and $y$ directions is denoted by $\Delta x$ and $\Delta y$, respectively.

Unlike the regular wave equation, the convective wave equation yields difficulties in obtaining accurate schemes due to the presence of the mixed derivative term $\phi_{xt}$. A scheme that is second-order accurate in space and in time was obtained using the following finite difference approximations:

$$(\phi_{tt})^n_{i,j} = \frac{\phi^{n+1}_{i,j} - 2\phi^n_{i,j} + \phi^{n-1}_{i,j}}{\Delta t^2} \tag{39}$$

$$(\phi_{tx})^n_{i,j} = \frac{\begin{pmatrix} 3\phi^{n+1}_{i,j} - 4\phi^{n+1}_{i-1,j} + \phi^{n+1}_{i-2,j} \\ -3\phi^{n-1}_{i,j} + 4\phi^{n-1}_{i-1,j} - \phi^{n-1}_{i-2,j} \end{pmatrix}}{4\Delta t\, \Delta x} \tag{40}$$

$$(\phi_{xx})^n_{i,j} = \frac{\phi^n_{i+1,j} - 2\phi^n_{i,j} + \phi^n_{i-1,j}}{\Delta x^2} \tag{41}$$

$$(\phi_{yy})^n_{i,j} = \frac{\phi^n_{i,j+1} - 2\phi^n_{i,j} + \phi^n_{i,j-1}}{\Delta y^2}. \tag{42}$$

Note that all the second-order derivatives are evaluated using the standard central difference formula except the mixed derivative term. Here we use upwinding, as the central difference formula cannot be used for the mixed derivative term, since it results in an unstable scheme. It can be shown that the truncation error corresponding to this term is given by

$$\begin{aligned} \mathrm{ERROR}_{\mathrm{Truncation}} &= -\frac{\Delta t^2}{12}\phi_{tttt} - \frac{\Delta t^2}{3}\phi_{tttx} \\ &\quad + \frac{2\Delta x^2}{3}\phi_{txxx} + \frac{\Delta x^2}{12}(c^2-1)\,\phi_{xxxx} \\ &\quad + \frac{\Delta y^2}{12}c^2\phi_{yyyy} + O(\Delta t^3) \\ &= O(\Delta t^2, \Delta x^2, \Delta y^2). \end{aligned} \tag{43}$$

Substituting Eqs. (39)–(42) into (27), we obtain the numerical scheme

$$\begin{aligned} &\phi^{n+1}_{i,j} - 2\phi^n_{i,j} + \phi^{n-1}_{i,j} \\ &\quad + 0.5R(3\phi^{n+1}_{i,j} - 4\phi^{n+1}_{i-1,j} + \phi^{n+1}_{i-2,j} \\ &\quad - 3\phi^{n-1}_{i,j} + 4\phi^{n-1}_{i-1,j} - \phi^{n-1}_{i-2,j}) \\ &\quad + (1-c^2)\,R^2(\phi^n_{i+1,j} - 2\phi^n_{i,j} + \phi^n_{i-1,j}) \\ &\quad - c^2R^2(\phi^n_{i,j+1} - 2\phi^n_{i,j} + \phi^n_{i,j-1}) = 0 \end{aligned} \tag{44}$$

where

$$R = \frac{\Delta t}{\Delta x} = \frac{\Delta t}{\Delta y}.$$

To discuss the stability of the scheme we let the error term be the form

$$E^t_{lj} = A\xi^t e^{i\alpha\Delta x l} e^{i\beta\Delta y j}. \tag{45}$$

Substituting into (44), we obtain the error equation

$$\begin{aligned} &\xi^2(1 + 1.5R - 2\mathrm{Re}^{-i\alpha\Delta x} + 0.5\mathrm{Re}^{-i2\alpha\Delta x}) \\ &\quad + \xi\left[-2 + 4(c^2-1)\,R^2\sin^2\left(\frac{\alpha\Delta x}{2}\right) \right. \\ &\quad \left. + 4c^2R^2\sin^2\left(\frac{\beta\Delta y}{2}\right)\right] \\ &\quad + (1 - 1.5R + 2\mathrm{Re}^{-i\alpha\Delta x} - 0.5\mathrm{Re}^{-i2\alpha\Delta x}) = 0. \end{aligned} \tag{46}$$

We solve this equation numerically for all possible $\alpha\,\Delta x$ and $\beta\,\Delta y$ for fixed $R$ and $c$, and find that the roots of the equation are all within the unit circle if the following stability criteria are satisfied: for $M_\infty = 0.8$, $R < 0.15$; for $M_\infty = 0.5$, $R < 0.12$, where $M_\infty = 1/c$.

Note that there are fictitious points, namely those points at $j = -1$, $j = N+1$, $i = -2, -1$, and $i = M+1$. Thus, the scheme given by Eq. (48) is valid only in the interior domain, and special treatment is required on the grid line corresponding to $i = 1$ near the upstream boundary ($i = 0$).

### 4.2. *Numerical Differencing Scheme*

The finite difference equations used to model the governing equation and various boundary conditions are presented below.

*Upstream boundary.* The calculation is begun at the left boundary, where the boundary condition is

$$\phi_t + \frac{1}{S(\theta)}[\cos(\theta)\,\phi_x + \sin(\theta)\,\phi_y] + \frac{\phi}{2rS(\theta)} = 0. \tag{47}$$

The differencing used at the left boundary is obtained using the notations

$$(r)_{0,j} = \sqrt{x_0^2 + y_j^2} \tag{48}$$

$$(\cos(\theta))_{0,j} = \frac{x_0}{r_{0,j}} \tag{49}$$

$$(\sin(\theta))_{0,j} = \frac{y_j}{r_{0,j}} \tag{50}$$

$$\frac{1}{S(\theta)} = \frac{1}{S_{0,j}} = \frac{x_0}{r_{0,j}} + \sqrt{c^2 - y_j^2/r_{0,j}^2}. \tag{51}$$

The finite difference equation for the boundary $i = 0$ is then given by

$$\phi_{0,j}^{n+1}=\frac{1}{1+\Delta t/4rS_{0,j}}\left\{\phi_{0,j}^{n}-\frac{R}{2r_{0,j}S_{0,j}}\right.$$
$$\times\left[x_0(-3\phi_{0,j}^n+4\phi_{1,j}^n-\phi_{2,j}^n)\right.$$
$$\left.\left.+y_j(\phi_{0,j+1}^n-\phi_{0,j-1}^n)+\frac{\Delta t}{2}\phi_{0,j}^{n-1}\right]\right\},$$
$$j=1 \text{ to } N-1. \tag{52}$$

*Airfoil surface.* At the surface of the airfoil the boundary condition is

$$v+\partial\phi/\partial y=0. \tag{53}$$

The corresponding difference equation is

$$\phi_{i,0}^{n+1}=\tfrac{1}{3}(4\phi_{i,1}^{n+1}-\phi_{i,2}^{n+1}+2v_{i,0}\,\Delta y),$$
$$i=M_1 \text{ to } M_2, j=0, \tag{54}$$

where $M_1$ is the $i$ index of the grid point at the airfoil leading edge and where $M_2$ is the $i$ index of the grid point at the trailing edge.

*Top boundary.* On the top boundary the far field boundary condition is

$$\phi_t+\frac{1}{rS(\theta)}(x_i\phi_x+y_{N-1}\phi_y)+\frac{\phi}{2rS(\theta)}=0, \tag{55}$$

where the difference approximations are

$$\phi_{i,N}^{n+1}=\frac{1}{1+(Ry_{N-1}/r_{i,N-1}S_{i,N-1})+(\Delta t/4r_{i,N-1}S_{i,N-1})}$$
$$\times\left\{\phi_{i,N}^{n-1}+\phi_{i,N-2}^{n+1}-\phi_{i,N-2}^{n-1}\right.$$
$$-\frac{R}{r_{i,N-1}S_{i,N-1}}$$
$$\times\left[2x_i(\phi_{i+1,N-1}^n-\phi_{i-1,N-1}^n)\right.$$
$$+y_{N-1}(-\phi_{i,N-2}^{n+1}+\phi_{i,N}^{n-1}-\phi_{i,N-2}^{n-1})$$
$$\left.\left.+\frac{\Delta x}{2}\phi_{i,N-2}^{n-1}\right]\right\} \tag{56}$$

for $i=1$ to $M-1, j=N$.

*Downstream boundary.* At the downstream boundary the far field condition is

$$\phi_t+\frac{1}{rS(\theta)}\left[(x_{M-1}\phi_x+y_j\phi_y)+\frac{\phi}{2rS(\theta)}\right]=0. \tag{57}$$

The finite difference approximation is then

$$\phi_{M,j}^{n+1}=\frac{1}{1+(Rx_{M-1}/r_{M-1,j}S_{M-1,j})+(\Delta t/4r_{M-1,j}S_{M-1,j})}$$
$$\times\left\{\phi_{M,j}^{n-1}-\phi_{M-2,j}^{n+1}+\phi_{M-2,j}^{n-1}\right.$$
$$-\frac{R}{r_{M-1,j}S_{M-1,j}}$$
$$\times\left[x_{M-1}(-\phi_{M-2,j}^{n+1}+\phi_{M,j}^{n-1}-\phi_{M-2,j}^{n-1})\right.$$
$$+2y_j(\phi_{M-1,j+1}^n-\phi_{M-1,j-1}^n)$$
$$\left.\left.+\frac{\Delta x}{2}\phi_{M-2,j}^{n-1}\right]\right\} \tag{58}$$

for $i=M, j=1$ to $N-1$.

*Wake boundary and corner points.* For the wake boundary condition, we make use of the fact that $\phi$ is an odd function of $y$, so that $\Delta\phi=\phi^+-\phi^-=2\phi^+$, where "+" and "−" denote quantities above and below the wake, respectively. The wake boundary condition (28) then becomes

$$\frac{\partial}{\partial t}\phi^+ +\frac{\partial}{\partial x}\phi^+=0, \tag{59}$$

and the difference equation is

$$\phi_{i,0}^{n+1}=\phi_{i,0}^{n-1}-R(\phi_{i+1,0}^n-\phi_{i-1,0}^n)$$
$$\text{for}\quad i=M_2 \text{ to } M-1, j=0. \tag{60}$$

For the last grid point in the wake ($i=M, j=0$), we use

$$\phi_{M,0}^{n+1}=\frac{1}{1+R}\left[\phi_{M,0}^n+\phi_{M-1,0}^n-\phi_{M-1,0}^{n+1}\right.$$
$$\left.+R(\phi_{M-1,0}^{n+1}+\phi_{M-1,0}^n-\phi_{M,0}^n)\right]. \tag{61}$$

Last, for the corner points $\phi_{M,N}$, $\phi_{0,N}$ we just take $\phi$ to be the average value of the two nearby points, i.e.,

$$\phi_{0,N}^{n+1}=0.5(\phi_{0,N-1}^{n+1}+\phi_{1,N}^{n+1}) \tag{62}$$
$$\phi_{M,N}^{n+1}=0.5(\phi_{M,N-1}^{n+1}+\phi_{M-1,N}^{n+1}). \tag{63}$$

## 5. CALCULATION OF THE UNSTEADY RESPONSE FUNCTION

For purposes of comparing numerical results with known solutions to the thin airfoil, gust response problems, we

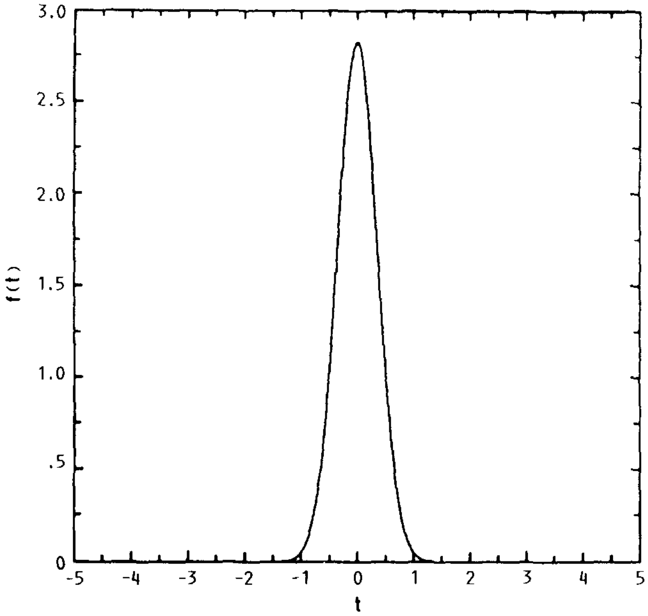


FIG. 4. Gaussian pulse.

introduce (following Sears [23]) the unsteady response function

$$R(k_1, M_\infty) = \frac{L}{\pi \rho l v_0 e^{(ivt)}}, \tag{64}$$

where $L$ is the unsteady lift, and $k_1$ ($k_1 = vl/2v_0$, where $v$ is the angular frequency of the incident disturbance) is the reduced frequency. The lift is calculated by integrating the unsteady pressure over the surface of the airfoil.

Since we solve the problem in the time domain, and not the frequency domain, we obtain the response function through the use of the Fourier transform. The upstream velocity disturbance is taken to be a wide band Gaussian pulse, and we obtain the airfoil response as a function of the reduced frequency as explained below.

Suppose that the value of the disturbance $v(x, y, t)$ at the center of the airfoil is $f(t)$. Then the time spectrum of this disturbance will be

$$F(\omega) = \frac{1}{\sqrt{2\pi}} \int_{-\infty}^{+\infty} f(t)\, e^{(i\omega t)}\, dt. \tag{65}$$

The response of the airfol to the disturbance will be

$$g(t) = \frac{L(t)}{\pi \rho c v_0}, \tag{66}$$

where the lift $L(t)$ is

$$L(t) = \int_\Gamma \tilde{p}(t)\, ds. \tag{67}$$

By taking the Fourier transformation of $g(t)$, we obtain the representation of $g(t)$ in the frequency domain $G(\omega)$, and the frequency response function of the airfoil is

$$R(\omega) = \frac{G(\omega)}{F(\omega)}. \tag{68}$$

For example, let us consider the case where

$$f(t) = \sqrt{2a}\, e^{(-at^2)}. \tag{69}$$

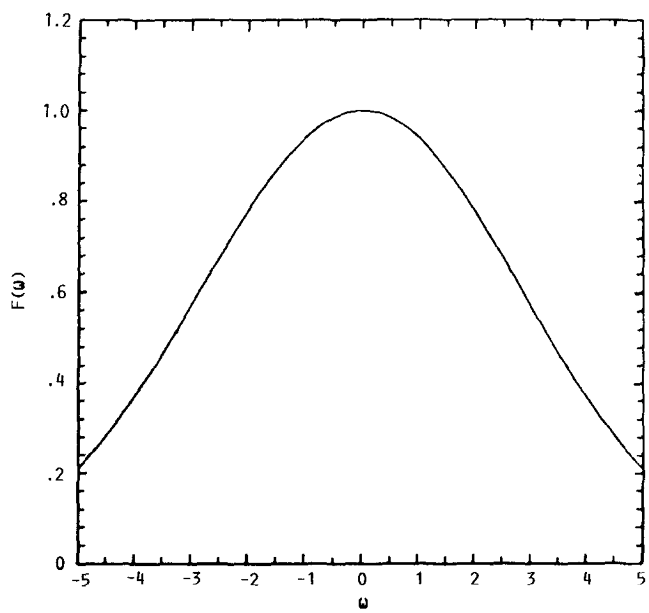


FIG. 5. Fourier transform of $f(t)$.

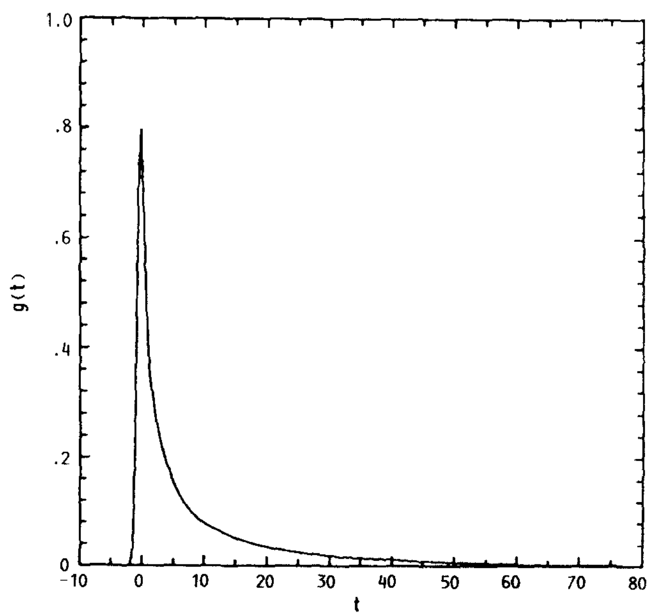


FIG. 6. Response function.

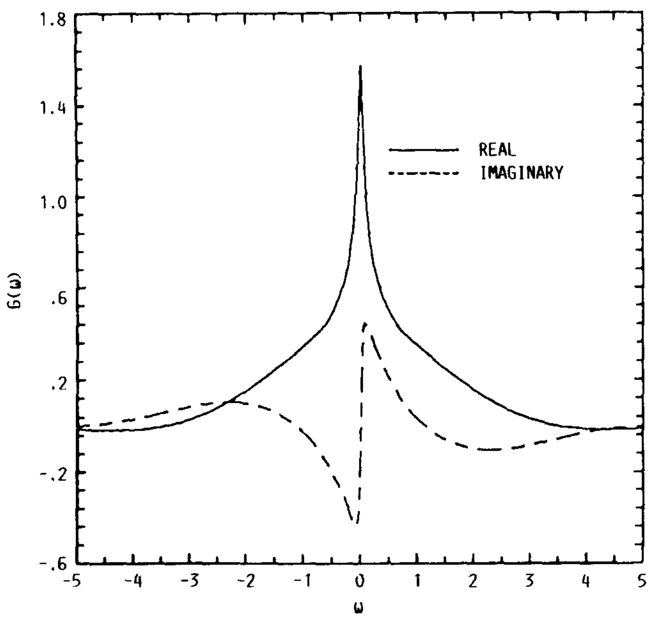


FIG. 7. Fourier transform of $g(t)$.

The spectrum of $f(t)$ is then

$$F(\omega) = e^{(-\omega^2/4a)}, \tag{70}$$

and the pulse function (disturbance) for the problem under consideration at time $t$ and at a point $x$ is $f(t-x)$.

The numerical integration involved in evaluating the transforms $F(\omega)$ and $G(\omega)$ depends on the value of the amplitude $a$. For example, for a value of $a = 4$, Fig. 4 shows the behavior of $f(t)$. Since the decay rate of this function is fast, one may choose a time interval of the form $[-T_0, T_0]$. A typical value of $T_0$ for our grids was 6.975. The corresponding transformation is given in Fig. 5. For numerical purposes, the index for the time begins at $t = -T_0$ so that $n = 0$ corresponds to $t = -T_0$. At the time level $n = 4000$, the pulse has passed the airfoil and the response function of $g(t)$ tends to zero. Therefore this is a good place to truncate the response function $g(t)$ numerically. We can then calculate its Fourier transformation $G(\omega)$ very easily using Riemann sums. The response function $g(t)$ and its transforms are given in Fig. 6 and 7, respectively. Finally, using (68), we obtain the frequency response function $R(\omega)$. The various frequency response functions given in Figs. 8–13 are obtained by plotting $\mathrm{Re}[R(\omega)]$ vs $\mathrm{Im}[R(\omega)]$.

## 6. RESULTS AND DISCUSSION

### 6.1. *Comparison of Numerical Results with Known Solutions*

In order to assess the accuracy of the present numerical scheme, we compare computed numerical results with known solutions to the thin airfoil gust response problem. Because the stability constraint of our scheme depends on the Mach number, we are limited to calculating cases for which the Mach number is not small. For comparison purposes we present results for Mach numbers of 0.5 and 0.8.

Figure 8 shows a comparison between analytical results obtained from a Possio [24] solver and numerical results obtained from the present scheme for a 0.5 Mach number. The grid dimensions for the results shown in Fig. 8 were 15 units in the streamwise direction and 10 units in the normal direction. The spacing in the $x$ and $y$ directions was uniform

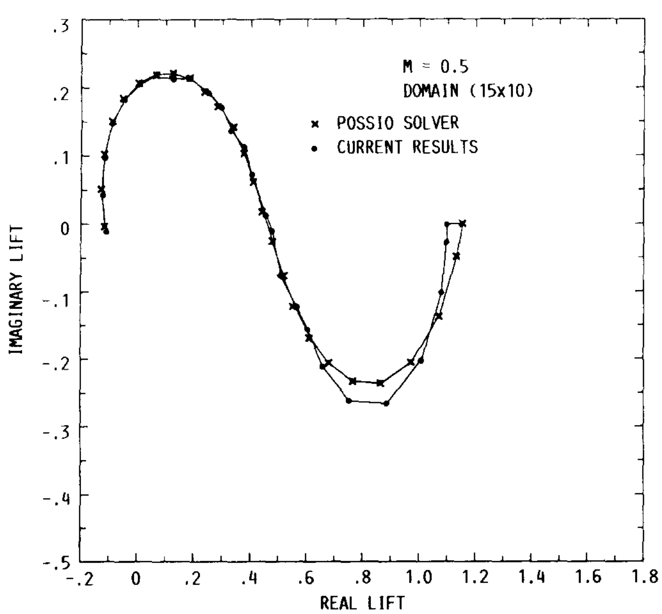


FIG. 8. Comparison between the numerically computed unsteady response function and analytical results from a Possio solver.

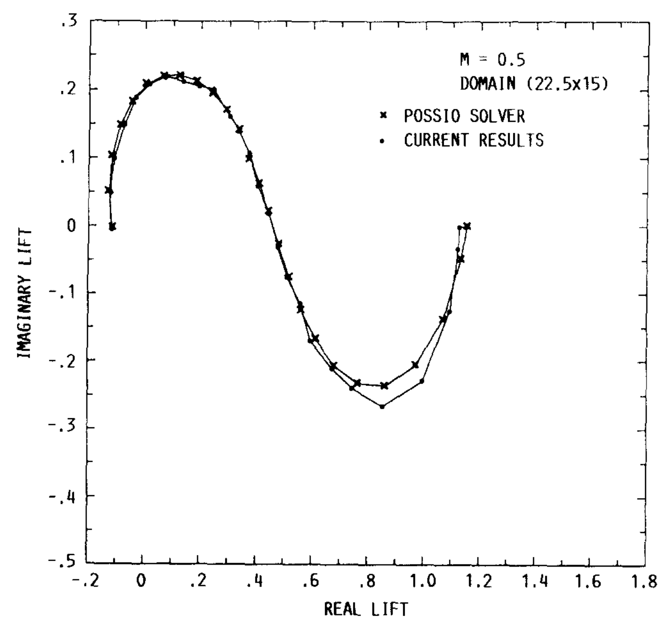


FIG. 9. Comparison between the numerically computed unsteady response function and analytical results from a Possio solver.

with $\Delta x = \Delta y$. There were 151 points in the $x$ direction and 101 points in the $y$ direction.

In Fig. 9 we make the same comparison as in Fig. 8, except that in this case the grid dimensions have been extended to 22.5 by 15. The number of grid points in each coordinate direction is the same as in Fig. 8, so that the spacing is slightly more coarse on this grid. The results shown in Fig. 10 were run on a still larger grid, with dimensions of 30 by 22.5, and 201 points in the $x$ direction and 151 points in the $y$ direction.

By comparing the results shown in Figs. 8–10, it is seen that the agreement for the high frequencies is very good in all three cases. However, the agreement for reduced frequencies below about 0.3 is only fair. Note that the amount of error in the low frequency cases diminishes as the grid dimensions become larger. This suggests that a larger grid is required to adequately model the long wavelength disturbances.

In Figs. 11–13 we present results for the case of an 0.8 Mach number. The grids used for these figures correspond to the grids used in Figs. 8–10, respectively. The agreement for the 0.8 Mach number case is analogous to the agreement for the 0.5 Mach number case, and again we see that the accuracy for lower frequencies is considerably improved on the larger grids.

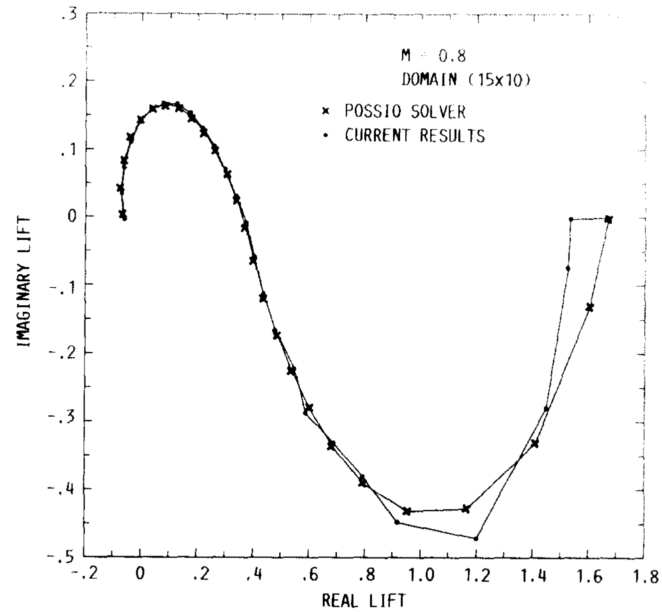


FIG. 11. Comparison between the numerically computed unsteady response function and analytical results from a Possio solver.

### 6.2. *Comparison of the Present Scheme with the Frequency Domain Approach of Scott and Atassi*

Scott and Atassi [14] have reported the development of a general frequency domain numerical scheme for the solution of periodic vortical flows around isolated airfoils. Their scheme has wide applicability to many different flow configurations and was recently extended to handle the difficult problem of vortical flows around lifting airfoils in subsonic flows [10, 15]. In the present section we compare the present time domain numerical scheme with their frequency domain approach as specialized to the case of flat plate airfoils.

There are two main disadvantages to the frequency domain approach reported in [14]. First, in the frequency

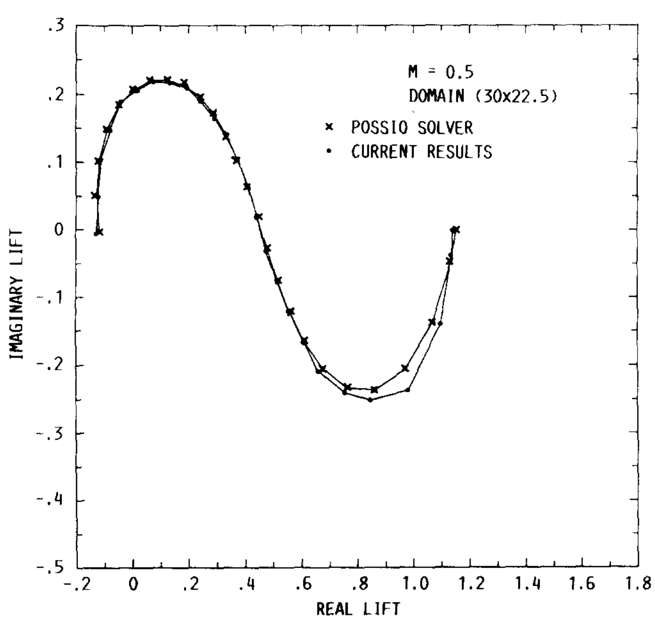


FIG. 10. Comparison between the numerically computed unsteady response function and analytical results from a Possio solver.

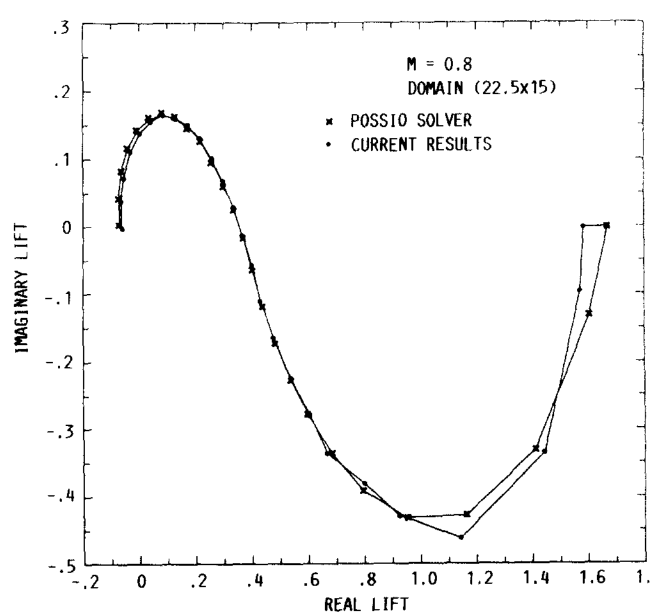


FIG. 12. Comparison between the numerically computed unsteady response function and analytical results from a Possio solver.

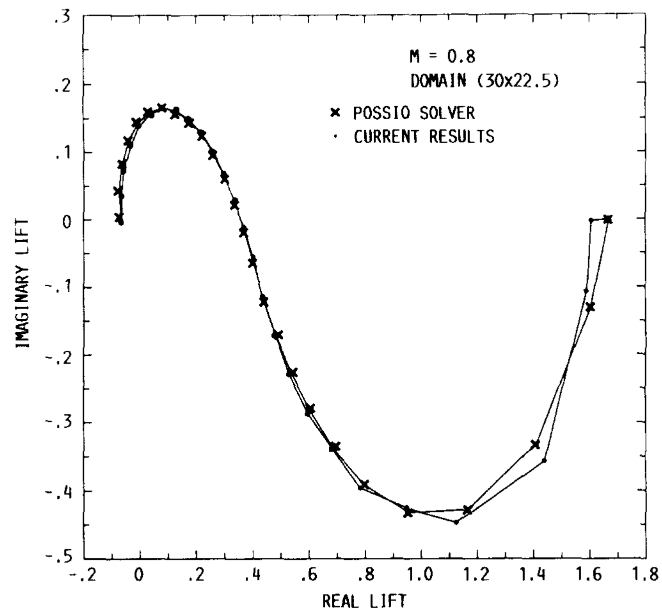


**FIG. 13.** Comparison between the numerically computed unsteady response function and analytical results from a Possio solver.

domain formulation it is necessary to solve the gust response problem in terms of discrete frequencies. For disturbances that contain many harmonics, many calculations would be necessary, and the frequency domain approach would be inefficient. Second, there is a loss of accuracy and an increase in solution times required for the higher frequencies. This makes the frequency domain approach ill-suited for reduced frequencies that are in the range of 10 or higher.

There are, nonetheless, significant advantages to the frequency domain approach reported in [14]. First, it is very accurate for a large range of frequencies, including the very lowest frequencies. Their scheme can be used for both incompressible and compressible flows and has been validated for three-dimensional gusts. In addition, the unsteady grid and far field boundary condition are ideally suited for acoustic wave propagation, so that the far field acoustics can be accurately and readily determined from the solution.

The chief advantages of the time domain scheme presented in this paper are that the scheme is very accurate at the higher frequencies and that it can handle general vortical disturbances without solving the problem in terms of discrete frequencies. The main disadvantages of the present approach are the loss of accuracy for the low reduced frequencies and the fact that it is not valid for low Mach number flows.

In terms of computational and storage efficiency, both approaches are far superior to standard primitive variable solvers. They both can be efficiently run on a present day work station. Sample solution times for calculating an entire response function using the time domain approach range from 86 to 343 s on a Cray X-MP versus 60 to 150 s for the same calculation using the frequency domain appraoch.

## 6.3. *Conclusion*

In conclusion, the time domain numerical scheme which has been developed in the present paper is both storage and computationally efficient and can accurately calculate the high frequency response of a flat plate airfoil in compressible flow to a transverse gust. Improvements are still needed in the accuracy of the calculation at the lower frequencies and in the selection of a more suitable computational grid.

In as much as nonlinear equations such as the Euler equations are usually solved using time marching procedures, it is hoped that the present time domain solution procedure for the linearized, unsteady Euler equations will illuminate some of the issues involved in time domain calculations for unsteady flows.

## REFERENCES

1. W. F. Ballhaus and P. M. Goorjian, *AIAA J.* **15**, 1728 (1977).
2. P. M. Goorjian, "Implicit Computations of Unsteady Transonic Flow Governed by the Full Potential Equation in the Conservation Form," AIAA Paper 80-0150, 1980 (unpublished).
3. N. L. Sankar, J. B. Malone, and Y. Tassa, "An Implicit Conservative Algorithm for Steady and Unsteady Three Dimensional Transonic Flows," AIAA Paper 81-1016, Palo Alto, CA, 1981 (unpublished).
4. P. M. Goorjian, and G. P. Guruswamy, "Unsteady Transonic Aerodynamic and Aeroelastic Calculations About Airfoils and Wings," NASA TM 85986, 1984 (unpublished).
5. J. M. Verdon and J. R. Caspar, *J. Fluid Mech.* **149**, 403 (1984).
6. W. J. McCroskey and P. M. Goorjian, "Interactions of Airfoils with Gusts and Concentrated Vortices in Unsteady Transonic Flow," AIAA Paper 83-1691, 1983 (unpublished).
7. W. J. McGroskey, *J. Aircraft* **22** (3), 236 (1985).
8. M. E. Goldstein and H. M. Atassi, *J. Fluid Mech.* **74**, 741 (1976).
9. H. M. Atassi, *J. Fluid Mech.* **141**, 109 (1984).
10. J. R. Scott and H. M. Atassi, "Numerical Solutions of the Linearized Euler Equations for Unsteady Vortical Flows Around Lifting Airfoils," AIAA Paper 90-0694, 1990 (unpublished).
11. J. R. Scott, "Compressible Flows with Periodic Vortical Disturbances Around Lifting Airfoils," Ph.D. dissertation, University of Notre Dame, April 1990 (unpublished).
12. M. E. Goldstein, *J. Fluid Mech.* **89** (3), 433 (1978).
13. H. M. Atassi and J. Grzedzinski, *J. Fluid Mech.* **209**, 385 (1989).
14. J. R. Scott and H. M. Atassi, "Numerical Solution of Periodic Vortical Flows about a Thin Airfoil," AIAA Paper 89-1691, 1989 (unpublished).
15. J. R. Scott and H. M. Atassi, in *Proceedings, Computational Fluid Dynamics Symposium on Aeropropulsion, Cleveland, Ohio, 1990*, NASA Conference Publication 10045 (unpublished).
16. B. E. Engquist and S. J. Osher, *Math. Comput.* **34**, 149, 45 (1980).

17. W. Whitlow, Jr., "XTRAN2L: A Program for Solving the General-Frequency Unsteady Transonic Small Disturbance Equation," NASA TM 85723, 1983 (unpublished).

18. H. M. Atassi, in *Proceedings of the Tenth U.S. National Congress of Applied Mechanics, 1986*, edited by J. P. Lamb (ASME, New York, 1986), 475.

19. H. M. Atassi and J. R. Scott, in *Proceedings of the Fourth International Symposium on Unsteady Aerodynamics and Aeroelasticity of Turbomachines and Propellers, Aachen, Germany, 1988*, edited by H. E. Gallus and S. Servaty (Institute für Strahlantriebe und Turbomachine, University of Aachen, Aachen), 39.

20. A. Bayliss and E. Turkel, *J. Comput. Phys.* **48**, 2 (1982).

21. F. G. Friedlander, *Proc. R. Soc. London Ser. A.* **269** (1962).

22. S. I. Hariharan and T. Hagstrom, "Far Field Expansions for Anisotropic Wave Equations," *Proceedings of the 2nd IMACS Symposium on Computational Acoustics, Princeton, NJ, 1989*, edited by D. Lee *et al.*

23. W. R. Sears, *J. Aerosp. Sci.* **81** (3) 104 (1941).

24. C. Possio, "L'Azione Aerodynamica sul Profilo Oscillante in un Fluido Compressible a Velocita Ipsonara," *L'Aerotechnica* **18** (4) (1938).